ACCSCIENCE PUBLISHING

Journal of Seismic Exploration

ARTICLE

Seismic characterization and spatial distribution analysis of coal gangue in the deep coalbed of the Northeastern Ordos Basin

Zelei Jiang[1,2]*, Xuri Huang[1,2,3,4], Dong Zhang[5], Yucong Huang[1,2], and Yong Wu[1,2]

[1]State Key Laboratory of Oil and Gas Reservoir Geology and Exploitation, School of Geosciences and Technology, Southwest Petroleum University, Chengdu, Sichuan, China

[2]United Research Institute of Seismic Acquisition and Imaging Method, School of Geosciences and Technology, Southwest Petroleum University, Chengdu, Sichuan, China

[3]Natural Gas Geology Key Laboratory of Sichuan Province, School of Geosciences and Technology, Southwest Petroleum University, Chengdu, Sichuan, China

[4]Key Laboratory of Piedmont Zone Oil and Gas Geophysical Exploration Technology for Petroleum and Chemical Industry, School of Geosciences and Technology, Southwest Petroleum University, Chengdu, Sichuan, China

[5]Department of Geophysical, Exploration and Development Research Institute, PetroChina Changqing Oilfield Company, Xi'an, Shaanxi, China

***Corresponding author:**
Zelei Jiang
(jiangzl9602@163.com)

Citation: Jiang Z, Huang X, Zhang D, Huang, Wu Y. Seismic characterization and spatial distribution analysis of coal gangue in the deep coalbed of the Northeastern Ordos Basin. *J Seismic Explor*. doi: 10.36922/JSE025490123

Received: December 4, 2025

Revised: January 21, 2026

Accepted: January 22, 2026

Published online: March 6, 2026

Abstract

Deep coalbed methane exploration in the Ordos Basin holds significant potential, yet the frequent development of coal gangue severely hinders productivity and complicates horizontal well deployment. Accurately characterizing the spatial distribution of these thin coal gangue layers remains a critical challenge, particularly when constrained by limited seismic resolution and sparse well control. To address this challenge, we propose a novel paleogeomorphology-constrained stochastic seismic inversion workflow applied to the Benxi Formation in the YL area. This approach integrates petrophysical analysis with paleogeomorphic restoration, identifying natural gamma as the most sensitive lithological indicator. Under hierarchical geomorphic constraints, geostatistical simulation was utilized to predict the three-dimensional spatial probability of coal gangue occurrence. Quantitative validation demonstrates a robust correlation between coal gangue thickness and natural gamma response, with the inversion results achieving an accuracy of 81.82% in blind well validation. Spatially, gangue development is controlled by paleotopography, with higher probabilities concentrated in paleo-highs and slopes associated with stronger hydrodynamic conditions, while paleo-depressions exhibit superior coal continuity. This study not only overcomes the resolution limitations of traditional inversion in sparse-well areas but also provides a rigorous quantitative geological basis for sweet-spot identification and trajectory optimization in deep coalbed methane development.

Keywords: Ordos Basin; Coal gangue-sensitive log parameter; Seismic characterization of deep coal gangue; Coal gangue distribution pattern; Deep coalbed methane

1. Introduction

In the Ordos Basin, coal-bearing strata were extensively developed in the Late Paleozoic transitional marine–continental environment. The main coalbeds, including the No. 5 coal of the Shanxi Formation (Lower Permian) and the No. 8 coal of the Benxi Formation (Upper Carboniferous), are rich in gas resources and represent the primary targets for deep coalbed methane (CBM) exploration. Unlike conventional CBM, coal-rock gas exhibits geological characteristics of high pressure, temperature, gas content, saturation, and free gas content.[1] Owing to differences in coal-forming periods and depositional environments, coal gangue layers commonly occur within deep coalbeds, which not only affect gas content but also complicate the design of horizontal well trajectories.[2]

Previous studies have investigated coal gangue identification and characterization mainly based on log data, sedimentological observations, and laboratory experiments. Guo *et al.*[3] reported that coal gangue generally exhibits higher density and natural gamma (GR) responses than coalbed, reflecting their mudstone-dominated or siltstone-dominated compositions. Zhang *et al.*[4] further demonstrated that coal gangue appears as distinct dark bands on image logs, characterized by elevated thorium and uranium values, higher density, and lower resistivity compared with pure coalbeds. These logging indicators provide a foundation for distinguishing coal gangue from coal in vertical profiles.

From a reservoir perspective, Sun *et al.*[5] found that the spatial variability and complexity of coal gangue development strongly influence reservoir properties and gas-bearing capacity. Specifically, coal gangue increases ash yield, reduces methane adsorption capacity, disrupts coal continuity, and complicates coalbed structures, ultimately hindering CBM preservation and production. Considerable efforts have also been devoted to examining the mechanical effects of coal gangue layers and surrounding rocks. Li *et al.*[6] conducted numerical simulations and revealed that coal gangue thickness directly affects stress concentration within coal-bearing strata, influencing bed stability. Yan *et al.*[7] conducted rock mechanical experiments and stress-field modeling and reported that increasing coal gangue thickness reduces both the maximum horizontal stress and the overall stress difference, thereby altering hydraulic fracturing behavior and fracture propagation patterns. Huang *et al.*[8] analyzed stress distribution and failure characteristics in coal gangue composite strata and found that coal gangue tends to bear relatively higher horizontal stress owing to its greater mechanical strength.

With technological advances, computed tomography scanning has also been introduced for coal gangue identification. Gong *et al.*[9,10] systematically investigated the pressure-dependent elastic anisotropy of deep coal reservoirs by integrating microscopic observations, ultrasonic experiments, and anisotropic rock physics modeling, thereby providing reliable support for stress simulation applications in deep coal reservoirs. Wu *et al.*[11] conducted gas desorption experiments combined with multiscale pore structure analyses and found that soft coal exhibited more developed pore structures and better pore connectivity, thereby demonstrating that high-rank soft coal has a significantly higher initial gas desorption capacity than hard coal. Wu *et al.*[12] proposed a rapid method for determining residual gas pressure in pre-pumped coal seams based on adsorption–desorption equilibrium experiments, offering higher efficiency, fewer required parameters, and lower errors than conventional Langmuir-based indirect methods and direct downhole pressure measurements.

In addition, Zhang *et al.*[13] found that cyclic loading–unloading stress can significantly enhance the permeability of deep coalbed gas reservoirs, with the most pronounced effect observed in coal seams containing inclined fractures, providing an important mechanical basis for optimizing the extraction of complex coalbed gas. In another study, Huang *et al.*[14] used spiral computed tomography to achieve high-resolution detection of coal gangue layers and reported that coalbeds with lower coal gangue content and thinner single layers exhibit higher gas content and greater development potential. Yang *et al.*[15] proposed an attribute-fusion method integrating vibration signals with cross-optimal selection to improve coal gangue identification accuracy. In the Ordos Basin, Xu *et al.*[16] analyzed logs from the No. 8 coal and classified the coalbed into three structural types—single-split, double-split, and triple-split—providing essential insights into internal heterogeneity.

Although existing studies have characterized coal gangue properties from various perspectives, research integrating paleogeomorphology, log, and seismic inversion to reveal its three-dimensional (3D) spatial distribution remains limited, highlighting the necessity of the present work.

Overall, existing studies on coal gangue have primarily focused on log-based identification, pore structure characterization, and mechanical properties, whereas insufficient attention has been paid to the fine-scale spatial distribution of coal gangue at inter-well and regional scales. In particular, under a 3D geological framework, the continuity, heterogeneity, and spatial coupling between coal gangue distribution, paleogeomorphology, and depositional microfacies remain poorly constrained, limiting a comprehensive understanding of coal gangue development patterns and their implications for CBM accumulation and development. In practice, the coal gangue directly affects well trajectory design and perforation strategies for reservoir production.[17]

In this study, log and core data were employed to achieve high-precision classification of coal and gangues, with GR identified as the most sensitive parameter for coal gangue recognition. Seismic characterization was further applied to delineate the spatial distribution of coal gangue within the No. 8 coalbed. Combined with regional tectonic evolution and sedimentary facies analysis, the depositional features and distribution patterns of coal gangue were clarified, providing significant guidance for sweet-spot identification and horizontal well trajectory optimization in deep CBM development within the Ordos Basin.

2. Geological overview of the study area

The YL area (Yulin area) is situated in the northeastern part of the Yishan Slope within the Ordos Basin (Figure 1). The top boundary of the No. 8 coalbed in the Benxi Formation presents a gentle monocline structure dipping from east to west, reflecting the overall tectonic framework of the region. The burial depth of the coalbed gradually increases westward, ranging from 2,260 m to 3,250 m,[18] indicating progressive subsidence during the late Paleozoic. The No. 8 coalbed was deposited in a lagoon–tidal flat environment,[19] where relatively stable hydrodynamic conditions favored the accumulation and preservation of thick coal seams. This coalbed is widely distributed across the basin and hosts abundant CBM resources, making it a key target for exploration and development. Its thickness generally increases toward the east and decreases toward the southwest. In the central and eastern portions of the study area, the coalbed thickness ranges from 3 m to 12 m, with an average of 7.2 m.

Due to fluctuations in relative sea level, multiple short-term depositional cycles were developed within the Benxi Formation.[20] These cycles caused repeated transitions between coal-forming environments and mudflat sedimentation. Consequently, thin mudstone layers were frequently identified as coal gangue within the No. 8 coalbed, forming numerous coal gangue layers of varying thickness. These coal gangue layers display significant lateral and vertical variability, both between wells and within individual well profiles. Such variability results in rapid spatial changes in coalbed architecture, which significantly enhances reservoir heterogeneity.[21] The distribution and continuity of these coal gangue layers not only affect the mechanical properties of the coalbed but also exert a substantial influence on its internal permeability structure and CBM enrichment patterns. Understanding their spatial characteristics is therefore crucial for accurately predicting reservoir

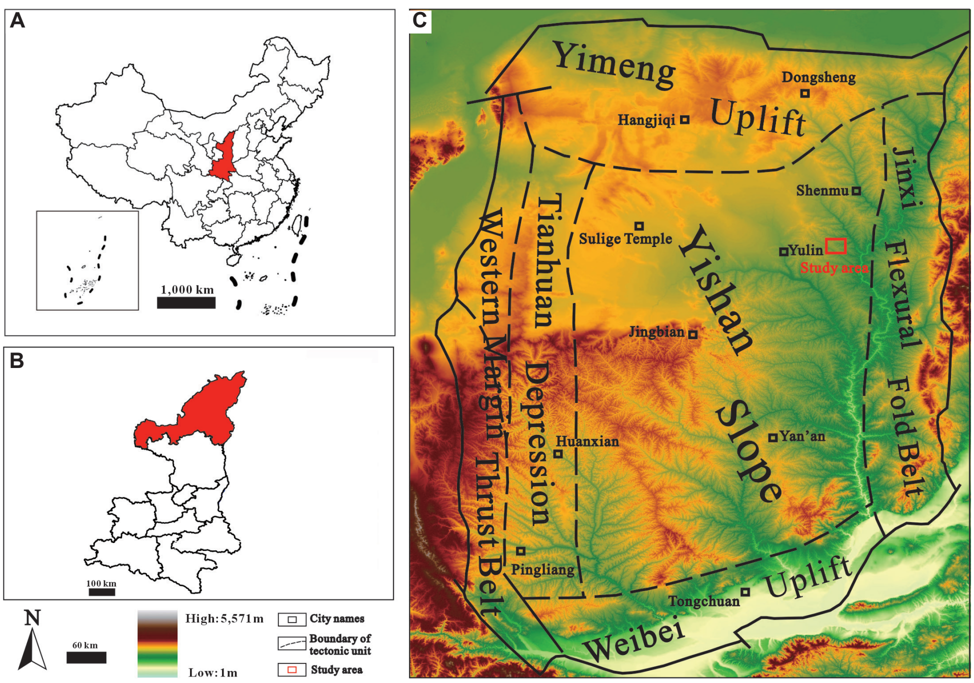

Figure 1. Location map of the study area. (A) Location of Shaanxi Province in China. (B) Location of the YL work area in Shaanxi Province. (C) Location of the YL work area in the elevation map of the Ordos Basin.

quality and optimizing CBM development strategies in the YL area.

The target zone of this study was the Carboniferous Benxi Formation, deposited in a characteristic marine–continental transitional environment. Drilling data and comprehensive log interpretations indicate that its lithology is dominated by sandstone, coal, dark mudstone, and locally developed limestone. To better understand the internal architecture of the coal-bearing strata, the vertical lithologic assemblages within the target zone were systematically analyzed based on regional sedimentary evolution patterns combined with detailed well and log responses. As shown in Figure 2, the Benxi Formation mainly represents a tidal-flat subfacies system, characterized by frequent shifts in hydrodynamic conditions and repeated alternations of clastic and organic-rich deposits.

The coalbeds within the zone display distinctive log signatures, including low GR, density, and acoustic velocity, which collectively reflect their high organic content and relatively weak compaction. In contrast, limestone exhibits the highest velocity and density among all lithologies due to its strong cementation and carbonate composition. Sandstone and mudstone share relatively similar density and velocity ranges. However, they can be effectively differentiated using GR values, with sandstone typically showing significantly lower gamma responses. Coal gangue, primarily composed of thin interbedded mudstone, exhibits higher acoustic velocity and density than coalbeds and demonstrates logging characteristics similar to mudstone, enabling their identification through sensitive parameter comparison.

With the deepening exploration and large-scale development of deep CBM resources in the Ordos Basin, there is an increasing need for refined characterization of the internal structure, continuity, and spatial heterogeneity of coalbeds. In particular, the frequent occurrence of coal gangue layers poses significant challenges for reservoir evaluation, horizontal well drilling, and production performance prediction. Therefore, a systematic investigation into the spatial distribution and geological controls of coal gangue has become essential. Through the integrated analysis of sensitive log parameters, combined with seismic characterization, sedimentary evolution research, and facies interpretation, this study aims to elucidate the distribution patterns and controlling mechanisms of coal gangue within the Benxi Formation. The findings will provide a robust geological foundation and technical support for high-precision sweet-spot identification, optimized horizontal well placement, and the efficient development of deep CBM resources in the Ordos Basin.

3. Seismic characterization of deep coal gangue constrained by log patterns and paleogeomorphological boundaries

3.1. Analysis of log-sensitive parameters for coal gangue

Based on log data from six representative wells in the study area, combined with drilling and core data, detailed logging response analyses were conducted for both coalbed- and coal gangue-bearing intervals (Figure 3). Eight representative logging parameters were selected to systematically compare the petrophysical differences between coalbed and coal gangue layers and identify diagnostic response patterns that can reliably characterize coal gangue development.

The comparative analysis revealed that coal gangue layers generally exhibited a typical “five-high and three-low” log response pattern. Specifically, coal gangue showed high corrected gamma ray, density, acoustic velocity,

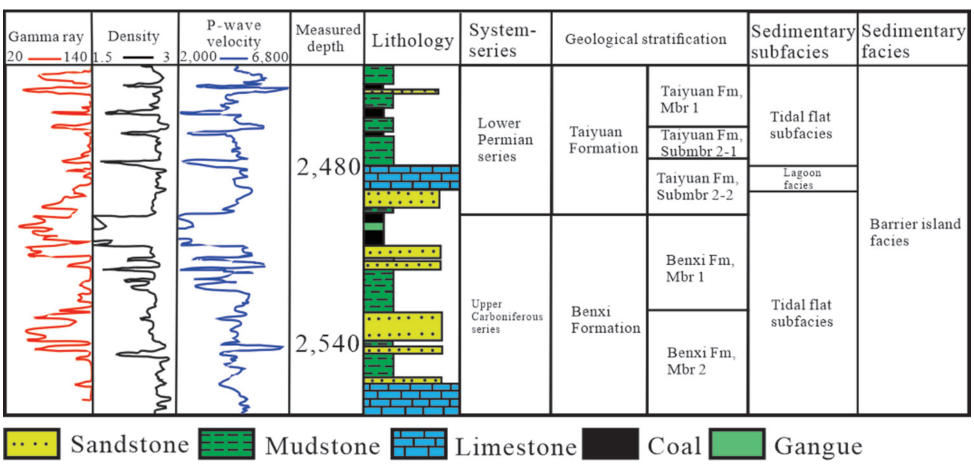

Figure 2. Representative well logging curves and the corresponding sedimentary facies map

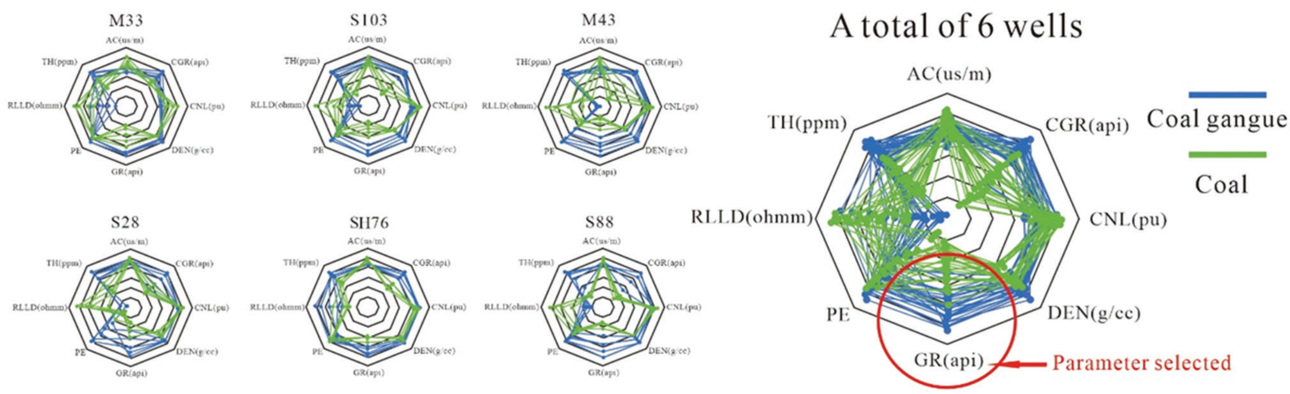

Figure 3. Comparison of log data-sensitive parameters between coalbeds and coal gangue. Radar charts for wells M33, S103, M43, S28, SH76, and S88 show sensitive log parameter responses for coal gangue layers in individual wells. The combined radar chart of all six wells presents the superimposed sensitive log parameter responses for coal gangue layers across all wells.

Abbreviations: AC: Acoustic transit time; CGR: Corrected gamma ray; CNL: Neutron porosity; DEN: Density; GR: Natural gamma; PE: Photoelectric absorption index; RLLD: Deep resistivity; TH: Thorium.

GR, and thorium content, accompanied by low deep resistivity, photoelectric absorption index, and neutron porosity. These characteristics reflect the higher clay and mud content of coal gangue, as well as their differences in mineral composition and pore structure relative to coal.

Among all parameters, the GR log demonstrated the highest sensitivity to coal gangue development. GR not only clearly differentiated mudstone coal gangue from coalbed but also provided stable and continuous responses across different wells. Compared with other indicators, GR showed the strongest correlation with the lithological variations observed in core samples, making it the most reliable parameter for delineating the thickness, boundaries, and spatial occurrence patterns of coal gangue layers. Therefore, GR was selected as the key sensitive attribute for subsequent seismic stochastic inversion aimed at generating the 3D probability volume of coal gangue distribution. This parameter choice ensures that the inversion results adequately reflect the vertical and lateral heterogeneity of coal gangue within the No. 8 coalbed, providing a solid foundation for subsequent reservoir characterization and sweet-spot prediction.

3.2. Probabilistic inversion of coal gangue spatial distribution

A 3D geological model of coalbeds and coal gangue provides a quantitative framework for characterizing their geological features and spatial distribution. It serves as an effective approach for fine-scale characterization of coal gangue and is also critical for optimizing horizontal well deployment and enhancing CBM development efficiency. By quantitatively characterizing coal gangue distribution in 3D space, such a model offers a more objective description of spatial patterns, thereby providing a robust basis for subsequent studies. Figure 4 shows the workflow of seismic characterization for coal gangue identification.

In geostatistical stochastic simulation, the two most critical tasks are: (i) Summarizing the statistical distribution of regionalized variables and (ii) Conducting variogram analysis. The variogram, as the fundamental tool of geostatistics, describes spatial correlation based on the principle that values at closer locations are more strongly correlated than those farther apart. The separation distance between two points is referred to as the lag (h), and the relationship between the variogram and lag distance h is illustrated in the variogram plot. Key parameters include the range, nugget, and sill (Figure 5). Common theoretical variogram models applied in geological modeling include the exponential, spherical, and Gaussian models, all of which asymptotically approach the sill.[22]

Among them, the Gaussian model gradually approaches the sill (c), reaching h = 0.95c in the range (a). This model is parabolic near the origin, making it the only variogram model with an inflection point. Its slope at the origin is zero, indicating very slow changes at short lag distances followed by rapid increases as the lag distance grows. The Gaussian model produces smoother and more continuous results at short ranges, but its overall stability is relatively lower compared with that of other models (**Equation 1**).

$$y(h) = c\left[1 - exp\left(-\frac{3h^2}{a^2}\right)\right] \quad (1)$$

Random simulation algorithms—constrained by input data—generate multiple geological realizations through stochastic functions while simultaneously considering

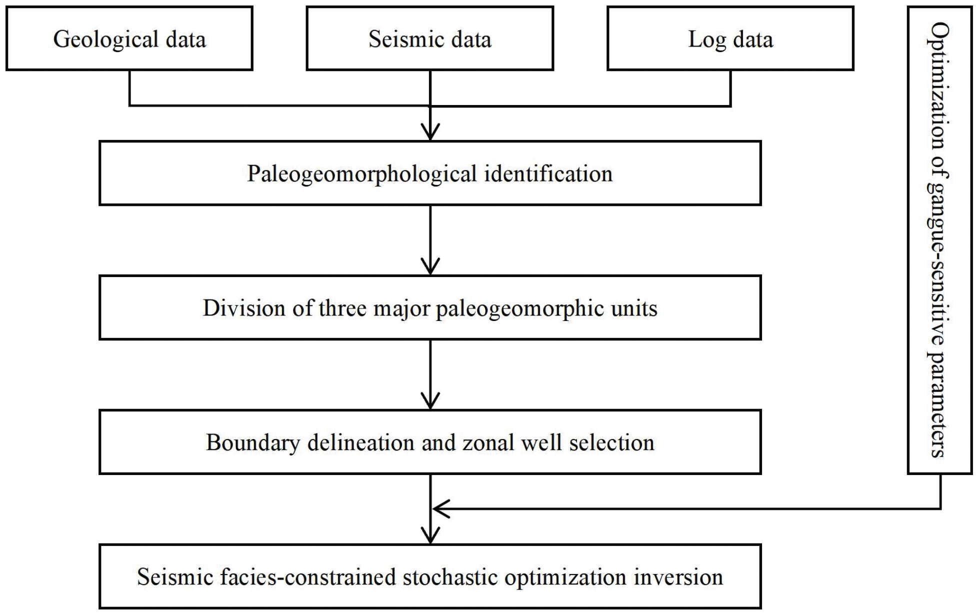

Figure 4. Workflow of seismic characterization of coal gangue

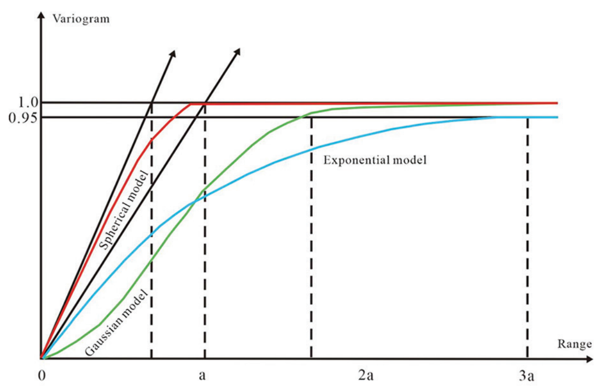

Figure 5. Common theoretical variogram models illustrating the relationship between variogram value and range

variable randomness and 3D space correlation. Sequential Gaussian simulation, a Kriging-based conditional simulation method for continuous variables, was applied in this study. The approach assumes that the input variables follow a Gaussian distribution and performs sequential simulation using Gaussian probability theory.

Before simulation, input data were detrended to conform to a standard normal distribution, and the final realizations were back-transformed to ensure consistency with the original data. In sequential Gaussian simulation, the study area is discretized into grids, and each grid node is simulated sequentially. At each node, the simulated value is determined by the mean and variance derived from the Kriging system and expressed as a cumulative conditional probability. Each realization of the regionalized variable $Z(x)$ is regarded as a random realization of the composite Gaussian distribution function $F(x)$, conditioned on n known data points $Z(x_i)$ ($i = 1, 2, ..., n$) and $m-1$ previously simulated values $Z(x_j)$ ($j = 0, 1, ..., m-1$). In subsequent work, sequential indicator simulation will be integrated with stochastic inversion results to construct the coal gangue model.[23]

In this study, well logs, 3D seismic, and geological data from the YL area were integrated. For the No. 8 coalbed of the Benxi Formation, GR was selected as the coal gangue-sensitive inversion parameter. The distribution pattern of GR and its correlation with coal gangue development were analyzed based on log data and geological data, from which a low-frequency trend and spatial structural model were established. Well constraints were introduced as prior conditions. A geostatistical stochastic optimization seismic inversion method was then applied, combining geostatistical simulation with seismic fitting.[24] This method primarily considers the probability density function of well log data.[25] Iterative updates were performed, preferentially re-simulating areas with larger mismatches while retaining well-fitted regions. This global–local alternating optimization ensures that the inversion simultaneously honors regional distributions and local structural variations.

After multiple iterations, a suite of equiprobable GR-based probability models for coal gangue distribution was generated (Figure 6). These models satisfy the following conditions: (i) Consistency with well logs and geostatistical characteristics; (ii) Amplitude and phase fitting of seismic data; and (iii) Coherence between global distribution patterns and local structures. The inversion results provided a robust foundation for quantitatively assessing the spatial distribution of coal gangue and analyzing the depositional evolution of the Benxi Formation coalbed in the YL area.

Based on seismic profile interpretation and stratigraphic horizon picking, the paleogeomorphic relief during the deposition of the No. 8 coalbed in the Benxi Formation was reconstructed. Through detailed structural analysis and seismic attribute extraction, the paleogeomorphic characteristics of the YL area were accurately identified. The resulting paleogeomorphic framework revealed distinct topographic differentiation, allowing the study area to be divided into three first-order geomorphic units with clearly defined boundaries. Figure 7A presents the 3D spatial display map, whereas Figure 7B shows the planar display map, displaying the following geomorphic units:

(i) Paleo-uplift area: Located in the western part of the study area, this zone is characterized by relatively high paleotopographic elevations, representing regions favorable for concentrated hydrodynamic energy and sediment bypass
(ii) Paleo-slope area: Situated between the uplift and the depression, this transitional zone displays a gentle east–west dip and serves as the main pathway for sediment transport from highlands to low-lying regions
(iii) Paleo-depression area: Distributed across the eastern part of the study area. This low-relief region exhibits lower elevations and provides favorable conditions for fine-grained sediment accumulation and coal-forming peat development.

The reconstructed paleogeomorphic pattern offers essential geological constraints for understanding coal gangue distribution and for guiding deep CBM exploration.

The thickness of the target coal-bearing strata is used as an important geological constraint for paleogeomorphic reconstruction. Thickness variations are interpreted to primarily reflect differential accommodation space controlled by paleotopography under relatively stable sediment supply conditions. In the study area, systematic lateral variations in coal-bearing strata thickness reveal clear paleogeomorphic differentiation, with thicker successions corresponding to paleo-depressions and thinner successions associated with paleo-uplift or slope settings.

Based on Table 1, the paleogeomorphic configuration during the coal deposition period exerted a significant control on the generation and spatial distribution of coal gangue. Paleo-depression areas exhibited the lowest coal gangue frequency and were characterized by relatively continuous, intact coalbeds, making them favorable zones for subsequent drilling and development.

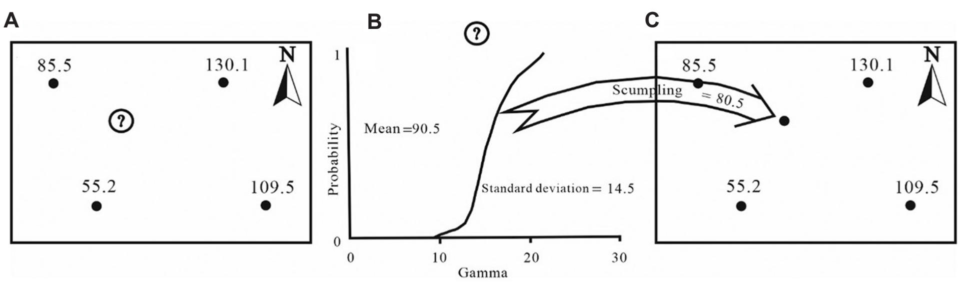

Figure 6. Schematic diagram of the stochastic simulation process. (A) Conditional data and locations to be simulated. (B) Grid node location. (C) Simulated value.

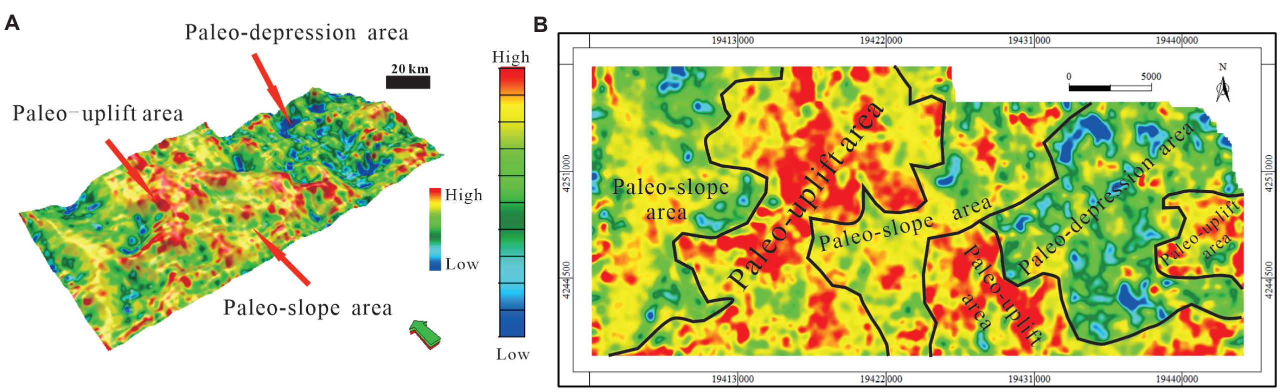

Figure 7. Paleogeomorphic region classification: (A) Three-dimensional visualization and (B) plan view

Conventional seismic inversion methods are often limited in complex depositional environments due to insufficient low-frequency information, and inversion constrained only by single wells suffers from uncertainties in low-frequency trend simulation, thereby affecting the accuracy of geological interpretation. To improve inversion precision, paleogeomorphic unit boundaries were introduced as constraints, serving as a crucial link between well data and depositional settings. By applying zonal constraints based on the three paleogeomorphic units, multi-scale control of seismic inversion was achieved.

In practice, inversion was performed using paleogeomorphic unit boundaries as geological control units, integrating well and seismic data for zoned inversion. Independent inversion calculations were performed for wells within different unit backgrounds. This approach preserved the lateral resolution of facies variations while effectively avoiding the "averaging effect" caused by excessively large vertical time windows, thereby significantly enhancing the fine-scale prediction capability of coal gangue distribution.

It should be noted that the zonal inversion applied to wells under different unit backgrounds refers to establishing inversion constraints separately within different paleogeomorphic zones, rather than spatially isolating the inversion calculations. All zones shared a unified inversion parameter system and the same initial model. This strategy ensures that the inversion results macroscopically adhere to regional geological depositional patterns while microscopically capturing local structural variations and heterogeneity, thereby significantly enhancing the spatial accuracy of coal gangue prediction in complex geological settings.

3.3. Blind-well validation using log data

Figure 8A illustrates the interpreted spatial distribution of coal gangue within the No. 8 coalbed based on log and well data, representing the actual geological configuration revealed by subsurface data. In comparison, Figure 8B displays the coal gangue probability map generated by the stochastic inversion results. Overall, the two maps show strong agreement in terms of spatial distribution patterns, lateral continuity, and the extent and location of major coal gangue-enriched zones. Areas with higher predicted coal gangue probability correspond closely to intervals confirmed by drilling to contain frequent coal gangue. This strong consistency validates the reliability and accuracy of the inversion method and indicates that the paleogeomorphically constrained inversion effectively captures the internal heterogeneity of the coalbed.

Table 1. Number of coal gangue layers in wells within the three paleogeomorphic areas

Paleogeomorphic area	Number of coal gangue layers (well-based statistics)	Proportion of total wells in the area (%)
Paleo-depression area	14	12.6
Paleo-slope area	33	42.3
Paleo-uplift area	52	64.9

Compared with multi-well interpolation results, which indicate consistent trends and more developed coal gangue in paleogeomorphic high areas, the lithofacies prediction based on 11 validation wells achieved an accuracy of 81.82% (Table 2). The discrepancies were mainly attributed to the extremely thin coal gangue layers, which may lead to misclassification.

To further validate the reliability of the inversion, a comparative analysis was conducted using seismic profiles and well-to-well correlation sections. Typical seismic sections of inversion parameters were compared with corresponding interpreted sections (Figure 9), and multi-well geological correlation profiles constructed were examined against inversion results (Figure 10). The validation results confirm that the predicted coal gangue locations, thicknesses, and trends closely match log-derived observations. This demonstrates the applicability of the stochastic optimization inversion method in the study area and confirms its accuracy in predicting coal gangue spatial distribution, thereby providing strong technical support for subsequent geological and reservoir analyses.

It is important to note that sparse well spacing has a significant impact on the lateral uncertainty of the prediction results. Since stochastic simulation relies on variograms to characterize spatial correlation, prediction uncertainty typically increases linearly with distance from well control points. In regions with relatively stable depositional environments, such as paleo-depressions, the error introduced by sparse well control is relatively minor. However, in highly heterogeneous transition zones, such as paleo-slopes, excessive inter-well spacing may limit the model's ability to capture high-frequency lithological variations. Therefore, the current prediction results (81.82% accuracy) represent the optimal estimation under existing well constraints, and data from future infill drilling are expected to further reduce lateral prediction uncertainty.

To address the limitation that stochastic inversion struggles to resolve thin layers due to seismic tuning thickness, future work will move beyond traditional statistical methods and focus on multi-attribute seismic pattern recognition. We plan to introduce machine learning algorithms, such as random forest or convolutional neural networks, to extract frequency-dependent attributes sensitive to thin layers and texture attributes sensitive to lithological boundaries. In addition, we aim to enhance the identification capability for the "weak gangue signatures" described in the present study through non-linear mapping in high-dimensional feature space, thereby achieving a more refined characterization of subtle geological bodies under seismic resolution constraints.

4. Discussion

The Ordos Basin is a multi-cycle superimposed petroliferous basin with a basement of Archean–Paleoproterozoic metamorphic rocks. Structurally, it is an asymmetric north–south-trending rectangular basin, characterized by a steep and narrow western margin and a broad, gentle eastern margin. As illustrated in Figure 11, the basin has undergone five stages of tectonic and sedimentary evolution. The first stage occurred during Mesoproterozoic–Neoproterozoic rifting, dominated by large-scale intracontinental and marginal crustal disintegration. The second stage was the Early Paleozoic marginal marine basin stage, with relatively stable vertical movements and marine sedimentary deposition. The third stage was the Late Carboniferous–Middle Triassic intracratonic basin stage, during which the basin evolved from a cratonic epicontinental sea to an intracratonic depression, with sedimentation transitioning

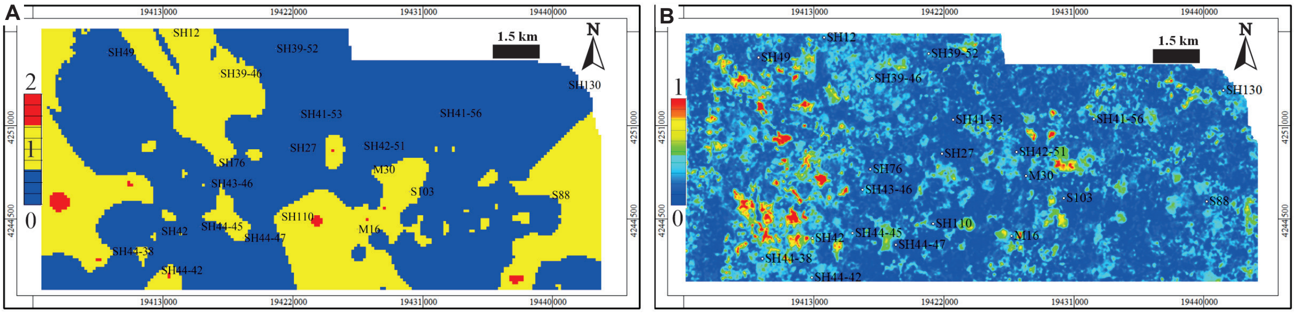

Figure 8. Spatial distribution of coal gangue. (A) Observed coal gangue based on log data and (B) predicted coal gangue probability distribution.

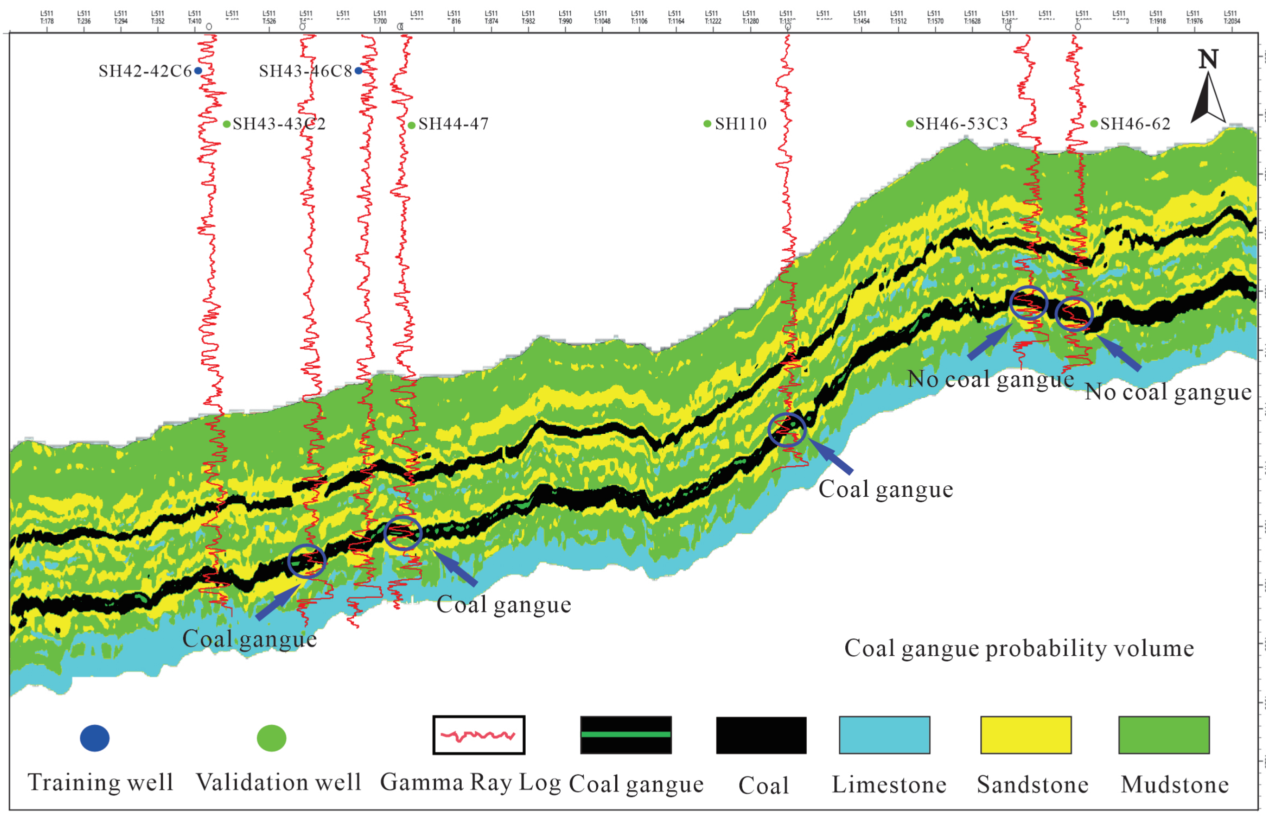

Figure 9. Seismic blind well profile verification

from marine–terrestrial transitional facies to lacustrine deposits. The fourth stage, spanning the Late Triassic and Early Cretaceous, was characterized by residual cratonic basin development, intense peripheral tectonism, thrust–fold deformation, tilting uplift, and regional unconformities between Triassic and Jurassic strata. During the Middle–Late Triassic extension, lacustrine systems reached their maximum development, depositing thick, high-quality source rocks. The fifth stage was the peripheral fault–depression stage, in which the basin shifted from subsidence to uplift and was subsequently segmented by faulting.[26,27]

Table 2. Comparison of observed and predicted coal gangue in wells and match status

Validation well	Observed coal gangue	Predicted coal gangue	Match status	Accuracy
SH43-43C2	Yes	Yes	Match	81.82%
SH42	Yes	No	Mismatch	
SH49	Yes	Yes	Match	
SH44-38	Yes	No	Mismatch	
SH44-41	Yes	Yes	Match	
SH46-62	No	No	Match	
SH44-47	Yes	Yes	Match	
SH46-53C3	No	No	Match	
M16	Yes	Yes	Match	
SH110	Yes	Yes	Match	
M30	Yes	Yes	Match	

Despite experiencing multiple tectonic movements throughout geological history, the Ordos Basin has remained structurally stable overall, characterized by the absence of large-scale active faults and relatively gentle deformation. Based on its current structural framework, the basin can be subdivided into six primary tectonic units: (i) The Yimeng Uplift in the north, (ii) The Weibei Uplift in the south, (iii) The Yishan Slope in the central part, (iv) The Jinxi Flexural Fold Belt to the east, (v) The Tianhuan Depression to the west, and (vi) The western thrust belt.

Among these, the Yishan Slope is the most extensive and significant unit, exerting a fundamental control on hydrocarbon enrichment patterns across the basin.[28] The Yishan Slope, developed during the late Early Cretaceous, forms a broad, gently west-dipping monocline extending approximately 400 km from north to south and 250 km from east to west. Its dip angle is typically <1°, although local structural variations, such as nose-like uplifts and minor warping, occur due to subtle tectonic adjustments.

The combination of wide areal extent, mild structural inclination, and high stability has made the Yishan Slope the principal zone for oil, gas, and CBM accumulation in the Ordos Basin. Under this gentle and stable tectonic background, sedimentation during the Early Carboniferous to Permian periods was dominated by epeiric sea environments. The initial transgression facilitated the deposition of subtidal carbonates across extensive shallow-marine platforms. As relative sea level gradually regressed, depositional

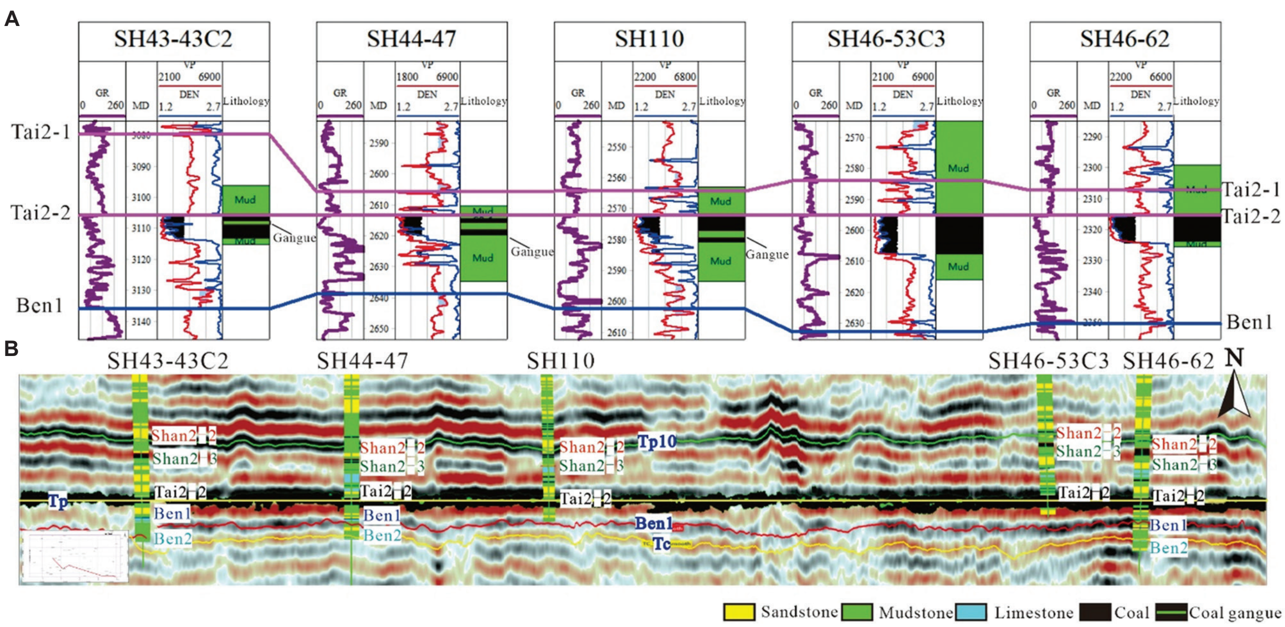

Figure 10. (A and B) Geological blind well cross-well profile verification

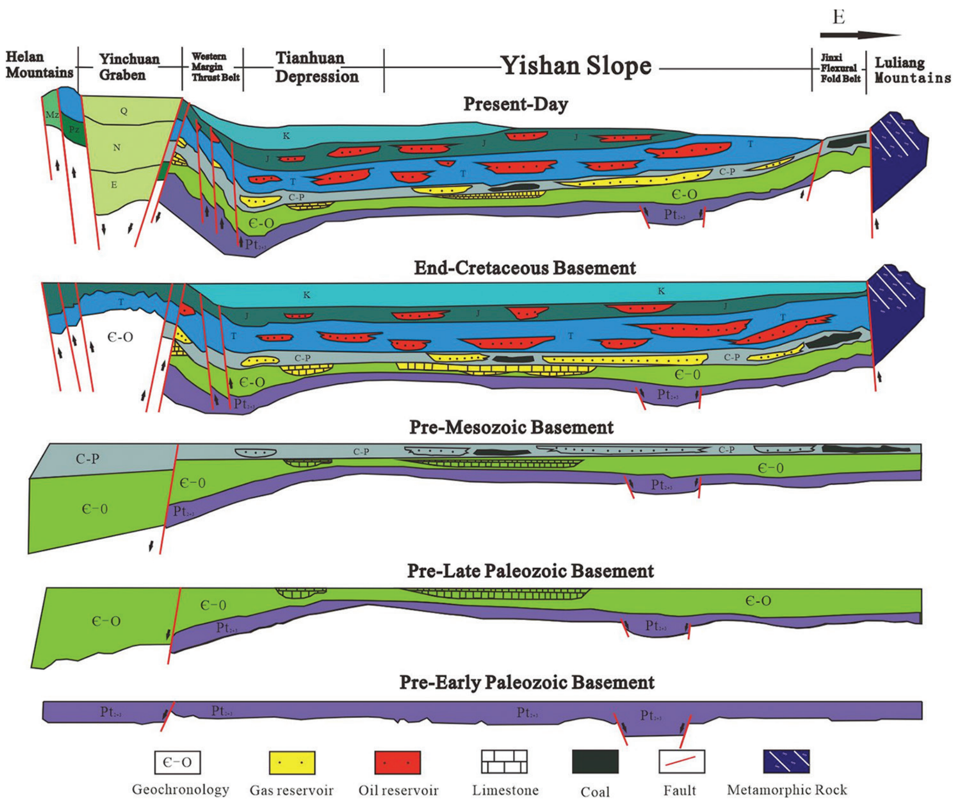

Figure 11. Structural sedimentary evolution profile of Ordos Basin. Adapted from Zhu *et al.*[27]

environments transitioned into delta-front terrigenous clastics, reflecting increasing continental influence. Toward the later stages, continued regression and shallowing resulted in the development of tidal-flat systems and widespread peat swamps. These conditions were highly favorable for the formation, preservation, and lateral continuity of thick and stable coalbeds (Figure 12). These long-lasting and relatively uniform depositional environments were essential for the extensive development of coal-bearing strata in the basin. The evolutionary sequence—from carbonate platform to clastic deltaic systems and finally to tidal-flat–peat complexes—provides key insights into the distribution, continuity, and internal heterogeneity of coalbeds, such as the No. 8 coalbed. Furthermore, the stability of the Yishan Slope ensured minimal tectonic disruption, allowing these coalbeds to maintain predictable structural patterns and making the region highly prospective for coal-related hydrocarbon resources.

The development of the No. 8 coal of the Benxi Formation in the YL area was controlled by the coupled effects of tectonics, climate, and sea-level change. During the Carboniferous period, the North China Plate was tectonically active, with peripheral orogeny inducing regional extension and facilitating epicontinental marine sedimentation. Under the background of Late Paleozoic glaciation, frequent glacial and interglacial cycles (1–2 Myr, with sea-level fluctuations of 50–100 m) periodically exposed coastal swamps, creating critical paleoclimatic conditions for extensive peat accumulation during the Benxi coal-forming period in North China.[29-31]

In the YL area, a key provenance reversal occurred between the Benxi 2 Formation and the Benxi 1 Formation. During the Benxi 2 Formation deposition, provenance was mainly derived from the northern Yinshan Uplift, resulting in quartzose sandstones associated with coalbeds. With the progressive uplift of the Qinling Orogenic Belt to the southeast, sediment supply during the Benxi 1 Formation shifted to the southeast, and depositional systems evolved into barrier coast and tidal-flat environments, favoring widespread development of organic-rich peat swamps. The prevailing warm and humid interglacial climate promoted lush vegetation growth and, coupled with slow subsidence, created favorable conditions for thick coalbed formation. High-frequency sea-level fluctuations induced dynamic hydrological changes, causing frequent vertical alternations of coal and mudstone, thereby generating coal gangue. Laterally, the No. 8 coal trends from southwest to northeast, thickening toward the northeast, with stable development of coalbeds up to 12 m thick in structural lows[32-34] (Figure 13). Thus, this tectonic–climate–sea-level coupling mechanism establishes a crucial sedimentary facies model for seismic prediction of coal gangue distribution in the YL area of the Ordos Basin.

Variations in hydrodynamic energy directly control the probability and thickness of coal gangue development. In paleo-highland and paleo-slope areas, relatively strong hydrodynamic conditions favor the input of fine-grained clastic materials, resulting in frequent coal gangue occurrences within coal seams. In contrast, paleo-depressions are dominated by peat accumulation, where coal gangue development is relatively minimal. Sediment supply modes also exert a primary control on the spatial distribution of coal gangue. Line-source supply systems (e.g., deltaic or barrier island systems) tend to generate laterally continuous thin coal gangue layers, whereas point-source supply systems (e.g., localized channels) are more likely to produce discrete or clustered coal gangue distributions. High-frequency sea-level fluctuations, as discussed earlier, periodically modulate accommodation space and sediment supply, leading to repeated alternations between peat accumulation and clastic deposition, thereby significantly enhancing coal gangue development within specific paleogeomorphic units.

By projecting the seismic-predicted coal gangue probability volumes onto the reconstructed paleogeomorphological framework, the spatial probability distribution of coal gangue within the No. 8 coalbed was systematically mapped (Figure 14). The integrated results revealed a strong and consistent correlation between coal gangue development and paleogeomorphological units. Coal gangue-prone areas are predominantly concentrated in regions characterized by medium to high paleotopographic relief, where stronger hydrodynamic conditions and variable sediment supply favored the deposition of mixed lithofacies. In contrast, low-relief paleodepressions exhibit significantly lower coal gangue probabilities, reflecting a sedimentary environment dominated by relatively stable water conditions and continuous peat accumulation.

This geomorphologically constrained probability mapping not only visualizes 3D inter-well coal gangue distribution but also elucidates the relationship between coal gangue occurrence and paleogeomorphic evolution. These findings highlight the controlling role of paleotopography in governing sediment transport pathways, depositional environments, and coal gangue formation mechanisms. From an engineering perspective, the results provide direct and practical guidance for deep CBM development. During well pattern deployment, areas with high coal gangue probabilities should be avoided to maintain coalbed continuity and ensure sufficient reservoir thickness. For horizontal well trajectory design, integrating the predicted coal gangue distribution enables optimization of drilling paths, reducing the likelihood of intersecting coal gangue. This approach increases effective coal exposure, enhances horizontal section stability, and ultimately improves gas deliverability and production efficiency.

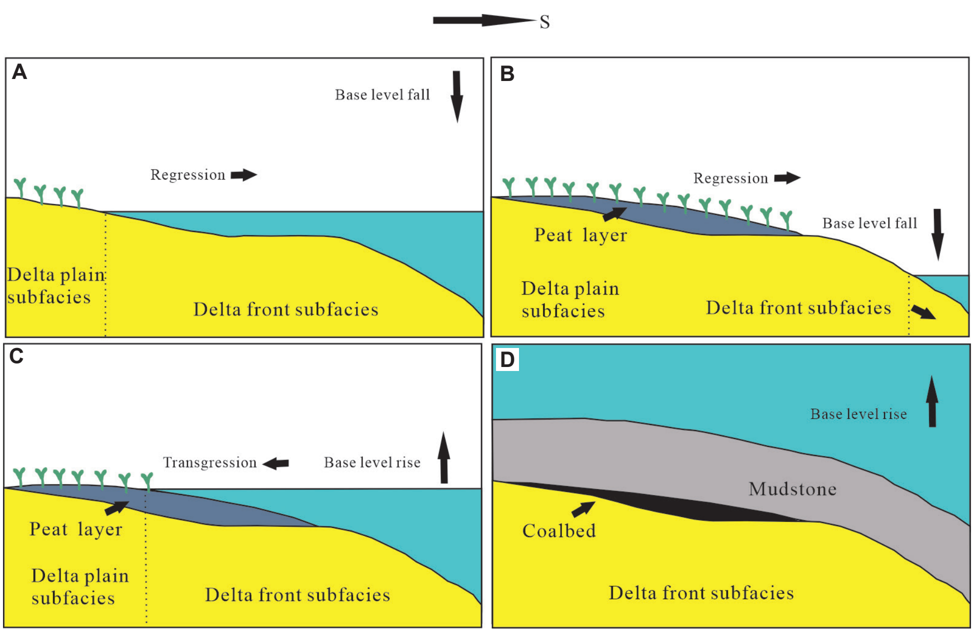

Figure 12. Coal accumulation model of the No. 8 coalbed in the Benxi Formation: (A) Early depositional stage of Mbr 1, Benxi FM (Late Carboniferous); (B) Late depositional stage of Mbr 1, Benxi FM (Late Carboniferous); (C) Late depositional stage of Mbr 1, Benxi FM (Late Carboniferous); (D) Depositional period of Taiyuan FM (Early Permian)

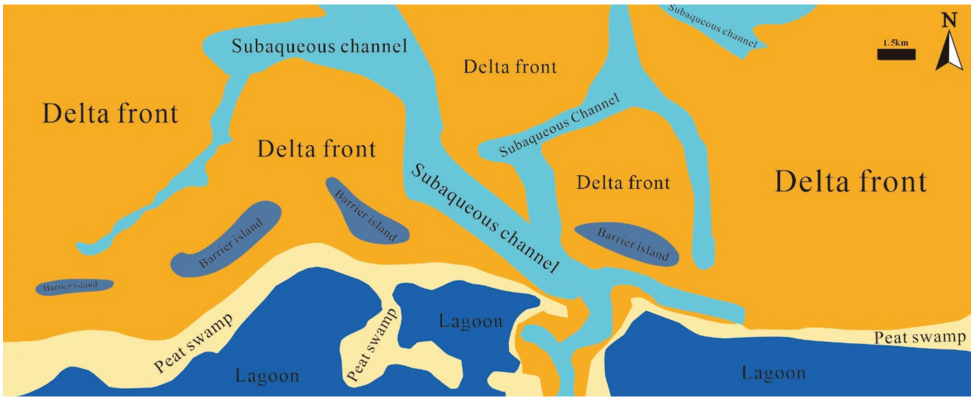

Figure 13. Sedimentary facies schematic diagram of the study area (before No. 8 coalbed deposition)

5. Conclusion

In predicting coal gangue, this study selected GR as the most sensitive log, and geostatistical stochastic optimization seismic inversion was performed to obtain the spatial probability volumes of coal gangue layers under paleogeomorphic zonation constraints. The predicted spatial distribution on maps, sections, and well-to-well profiles showed a high degree of consistency with log data, demonstrating strong geological reliability and engineering applicability. This confirms the robustness and practical value of the proposed method.

Based on geological, log, and geophysical data, the structural characteristics and sedimentary facies assemblages of the No. 8 coalbed in the Benxi Formation of the YL study area were clarified. The paleogeomorphology of the study area was identified as higher in the west and lower in the east, revealing a depositional evolution pattern in which the coalbed thickness gradually increases from west to east.

The geological features and spatial distribution of coal gangue in the YL area were clarified, and a strong coupling relationship between paleogeomorphology and coal gangue development was established, with an accuracy of 81.82%. Low-relief paleogeomorphological zones correspond to the lowest probability of coal gangue occurrence, making them favorable targets for coalbed development. Overall, by delineating the spatial distribution of coal gangue and interpreting its genetic and depositional controls, this study provides reliable theoretical support and technical guidance for the efficient exploration and development of deep CBM resources in the Ordos Basin.

Acknowledgments

We thank PetroChina Changqing Oilfield Company for permitting us to use their log and seismic data in this study.

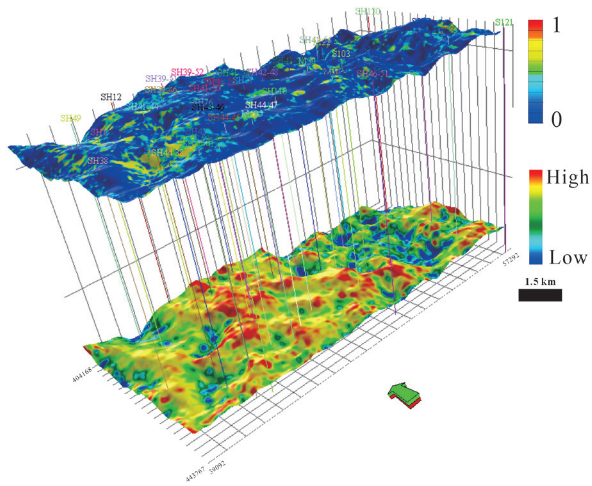

Figure 14. Three-dimensional display of coal gangue probability distribution projected onto paleogeomorphology

Funding

This study was supported by the Sichuan Science and Technology Program (No. 2025ZNSFSC0004), the National Natural Science Foundation of China (No. 42241206), and the National Natural Science Foundation of China (No. U24B2022).

Conflict of interest

The authors declare that they have no known financial or personal conflicts of interest that could have influenced the work reported in this paper.

Author contributions

Conceptualization: Yucong Huang
Data curation: Yucong Huang
Formal analysis: Zelei Jiang
Funding acquisition: Xuri Huang
Methodology: Zelei Jiang
Project administration: Dong Zhang

Resources: Xuri Huang
Supervision: Xuri Huang, Dong Zhang, Yong Wu
Validation: Zelei Jiang
Visualization: Zelei Jiang
Writing–original draft: Zelei Jiang
Writing–review & editing: Zelei Jiang, Xuri Huang

Availability of data

The data in this study are not openly available as they are confidential data provided by PetroChina Changqing Oilfield Company.

References

1. Li G, Jia C, Zhao Q, Zhou T, Gao J. Coal-rock gas accumulation mechanism and the whole petroleum system of coal measures. *Pet Explor Dev*. 2025;52(1):33-49.

   doi: 10.1016/S1876-3804(25)60003-6

2. Li S, Wang C, Wang H, *et al*. Reservoir forming characteristics and favorable area evaluation of deep coalbed methane in Daning-Jixian Block. *Coal Geol Explor*. 2022;50(9):59-67.

   doi: 10.12363/issn.1001-1986.21.12.0842

3. Guo G, Liu Y, Wang C, Lv Y, Zhu X, Han G. Jiyu meiceng "san jiegou" de meiyan pinzhi zonghe pingjia [Comprehensive evaluation of coal rock quality based on "three structures" of coal seam]. *China Offshore Oil and Gas*. 2022;34(2):35-41.

   doi: 10.11935/j.issn.1673-1506.2022.02.004

4. Zhang L, Cai W. Mei cengqi chengxiang cejing ziliao zonghe pingjia fangfa [The evaluation method of imaging well logging data in coalbed methane reservoir]. *Well Log Technol.* 2009,33(6):571-574.

   doi: 10.3969/j.issn.1004-1338.2009.06.016

5. Sun B, Zeng F, Li M, Qi F. Xishan meitian malan kuangqu 8 hao mei jiqi jiagan de weiliang yu xitu yuansu diqiu huaxue tezhen [Geochemistry characteristics of trace elements and rare earth elements(REEs) of No. 8 coal and parting in Malan Coal Mine, Xishan Coalfield]. *J China Coal Soc.* 2010,35(01):110-116.

   doi: 10.13225/j.cnki.jccs.2010.01.002

6. Li Y. *Fuza Yingli Huanjing Han Jiagan Tehou Meiceng Dingmei Maoluo Guilv Ji Fangmei Gongyi Youhua [Caving Behavior of Top Coal and Optimization of Coal Drawing Technology in Extra-Thick Coal Seams with Gangue under Complex Stress Conditions*] China: China University of Mining and Technology; 2023.

7. Yan X, Xiong X, Xu F, *et al*. Shenbu meiyan chuceng dizhi lixue yingxiang jizhi ji kongzhi yinsu-yi eerduosi pendi daji qukuai weili [Deep coal geomechanical influence mechanism and its control factors of Daji Block in Ordos Basin]. *J China Coal Soc*. 2025;50(5):2550-2566.

   doi: 10.13225/j.cnki.jccs.2025.0037

8. Huang Q, Cheng J. Ruanying huceng yanti caichang diban de yingli fengbu ji pohuai tezheng yanjiu [Research on stress distribution and failure characteristics of coal mining floor in soft-hard alternant strata]. *Rock Soil Mech*. 2017,38(S1):36-42.

   doi: 10.16285/j.rsm.2017.s1.004

9. Gong F, Huang A, Kang W, *et al*. The influence of lamination and fracture on the velocity anisotropy of tectonic coals. *Geophysics*. 2024;89(6):MR355-MR365.

   doi: 10.1190/geo2024-0033.1

10. Gong F, Cheng J, Wang G, Peng S, Zhang Z. The effect of lamination on elastic anisotropy of primary coals under confining pressure: Experiment and theoretical modelling. *Geophys Prospect*. 2025;73(4):1228-1242.

    doi: 10.1111/1365-2478.70009

11. Wu K, Li S, Zhang H, *et al*. Initial characteristics of gas desorption in high-rank soft and hard coals and the causes of the differences. *ACS Omega*. 2025;10(30):33208-33219.

    doi: 10.1021/acsomega.5c03116

12. Wu K, Li S, Shi S, *et al*. A rapid method for the determination of coal seam gas pressure based on raw coal adsorption. *Energy Sci Eng*. 2025;13(10):4660-4673.

    doi: 10.1002/ese3.70258

13. Zhang L, Kan Z, Zhang C, Tian S, Zeng S, Hao D. Permeability and stress sensitivity of coals with different fracture directions under cyclic loading-unloading conditions: A case study of the Xutuan coal mine in Huaibei coalfield, China. *Rock Mech Rock Eng*. 2025;59(1):951-969.

    doi: 10.1007/s00603-025-04769-1

14. Huang H, Shi J, Chen G, *et al*. Eerduosi pendi daning-jixian qukuai shenceng bahaomei jiagan jiqi channeng guanxi fenxi [Analysis of the characteristics of interbedded gangue in the deep No. 8 coal seam of the Daning-Jixian block in the Ordos Basin and its relationship with production capacity]. *China Pet Explor*. 2025;30(4):108-119.

    doi: 10.3969/j.issn.1672-7703.2025.04.008

15. Yang Y, Zhang Y, Zeng Q. Research on coal gangue recognition based on multi-layer time domain feature processing and recognition features cross-optimal fusion. *Measurement*. 2022;204:112169.

    doi: 10.1016/j.measurement.2022.112169

16. Xu F, Nie Z, Sun W, *et al*. Eerduosi pendi dongyuan shenbu mei cengqi gaoxiao kaifa lilun jishu tixi [Theoretical and technological system for highly efficient development of deep coalbed methane in Daning-Jixian Block]. *J China Coal Soc*. 2024;49(1):528-544.

    doi: 10.13225/j.cnki.jccs.yh23.1290

17. Tang S, Tang D, Yang J, *et al*. Eerduosi pendi daning-jixian qukuai shenbu mei chuceng kongxi jiegou tezheng

ji chuceng qianli [Pore structure characteristics and gas storage potential of deep coal reservoirs in Daning-Jixian block of Ordos Basin]. *Acta Petrolei Sin*. 2023;44(11):1854-1866, 1902.

doi: 10.7623/syxb202311008

18. Xu F, Wang C, Xiong X, Xu B, Wang H, Zhao X. Eerduosi pendi dongyuan shenbu mei cengqi chengcang yanhua guilv yu kantan kaifa Shijian [Evolution law of deep coalbed methane reservoir formation and exploration and development practice in the eastern margin of Ordos Basin]. *Acta Petrolei Sin*. 2023;44(11):1764-1780.

doi: 10.7623/syxb202311002

19. Yan X, Xu F, Xiong X, *et al*. Shenbu mei cengqi kantan kaifa guanjian shiyan jishu ji fazhan fangxiang [Key experimental technologies and their development directions for the exploration and production of deep coalbed methane]. *Coal Geol Explor*. 2025;53(1):128-141.

doi: 10.12363/issn.1001-1986.25.01.0046

20. Zhang Y, Wu C, Li Y, *et al*. Coal-forming sedimentary model and its control on vertical reservoir heterogeneity of the upper carboniferous Benxi formation in Ordos basin, China. *Sci Rep.* 2025;15(1):28676.

doi: 10.1038/s41598-025-13928-x

21. Wang S, Duan L, Zhang M, Chen Z. Heterogeneity of coalbed methane pools and their exploration and development. *Pet Geol Exp.* 2000;22(4):368-370.

doi: 10.11781/sysydz200004368

22. Gong F, Zhang Z, Peng S, Guo Q, Wang G. Pre-stack seismic inversion of dual-porosity geometry in deep coalbed methane reservoirs based on decoupled equivalent medium theory. *Geophys Prospect*. 2026;74(1):e70131.

doi: 10.1111/1365-2478.70131

23. Wu Q, Xu H, Zou X. An effective method for 3D geological modeling with multi-source data integration. *Comput Geosci*. 2005;31(1):35-43.

doi: 10.1016/j.cageo.2004.09.005

24. Keith Turner A. Challenges and trends for geological modelling and visualisation. *Bull Eng Geol Environ*. 2006;65(2):109-127.

doi: 10.1007/s10064-005-0015-0

25. Yang Z, Lin C, Yin H, *et al*. Zhu chengfen fenxi zai Taizhong diqu aotaoxi yingshan zu tansuan yan yanxing shibie Zhong de yingyong [Application of principal component analysis in carbonate lithology identification of the Ordovician Yingshan Formation in Tazhong area]. *Nat Gas Geosci*. 2015;26(1):54-59.

doi: 10.11764/j.issn.1672-1926.2015.01.0054

26. Chong R, Yu X. Chuceng sanwei dizhi jianmo zhiliang kongzhi de guanjian dian [The keys to quality control of 3D reservoir modeling]. *Mar Geol Front*. 2011;27(7):64-69.

doi: 10.16028/j.1009-2722.2011.07.007

27. Zhu X, Deng X, Liu Z, Sun B, Liao J, Hui X. Daxing aoxian hupeng qianshui bianzhuang he sanjiaozhou chenji tezheng ji moshi: Yi eerduosi pendi longdong diqu yanchang zu weili [Sedimentary characteristics and model of shallow braided delta in large-scale lacustrine: An example from Triassic Yanchang Formation in Ordos Basin]. *Earth Sci Front*. 2013;20(2):19-28.

doi: cnki: sun:dxqy.0.2013-02-005

28. Wang J, Wang J. Low-amplitude structures and oil-gas enrichment on the Yishaan Slope, Ordos Basin. *Pet Explor Dev*. 2013;40(1):52-60.

doi: 10.1016/S1876-3804(13)60005-1

29. Zhao Z, Xu W, Zhao Z, *et al*. Geological characteristics and exploration breakthroughs of coal rock gas in carboniferous benxi formation, ordos basin, NW China. *Pet Explor Dev*. 2024;51(2):262-278.

doi: 10.1016/s1876-3804(24)60022-4

30. Cai Y, Gao G, Liu D, Qiu F. Eerduosi pendi dongyuan linxing zhongqu meixi qi fuji dizhi tiaojian ji chengzang moshi [Geological conditions for coal measure gas enrichment and accumulation models in Linxingzhong Block along the eastern margin of the Ordos Basin]. *Nat Gas Ind*. 2022;42(11):25-36.

doi: 10.3787/j.issn.1000-0976.2022.11.003

31. Jiang F, Jia C, Pang X, *et al*. Upper Paleozoic total petroleum system and geological model of natural gas enrichment in Ordos Basin, NW China. *Pet Explor Dev*. 2023;50(2):250-261.

doi: 10.1016/s1876-3804(23)60387-8

32. Li Y, Wu P, Gao J, *et al*. Mei cheng qi duoceng xi fuji jizhi yu quan hanqi xitong moshi-yi eerduosi pendi dongyuan linxing qukuai weili [Multilayer coal-derived gas enrichment mechanism and whole gas bearing system model: A case study on the Linxing Block along the eastern margin of the Ordos Basin]. *Nat Gas Ind*. 2022;42(6):52-64.

doi: 10.3787/j.issn.1000-0976.2022.06.005

33. Chen S, Tang D, Hou W, et al. Shenbu meiceng qi dizhi tiaojian teshu xing yu chuceng gongcheng xiangying [Geological particularity and reservoir engineering response of deep coalbed methane]. *Acta Petrolei Sin*. 2023;44(11):1993-2006.

doi: 10.7623/syxb202311018

34. Sun F, Zhou G, Tian W, Deng Z, Shen J. Meiceng qi xitong de dingyi'neihan'xingcheng ji yingyong-yi eerduosi pendi shitan xi-erdie xi meiceng weili [Definition, connotation, formation and application of coalbed methane system: A case study on the Carboniferous-Permian coal seams in the Ordos Basin]. *Nat Gas Ind*. 2024;44(7):42-53.

doi: 10.3787/j.issn.1000-0976.2024.07.004